Atmos. Chem. Phys., 11, 5897–5915, 2011
www.atmos-chem-phys.net/11/5897/2011/
doi:10.5194/acp-11-5897-2011

Atmospheric Chemistry and Physics

Aerosol ageing in an urban plume – implication for climate

P. Roldin[1], **E. Swietlicki**[1], **A. Massling**[1,*], **A. Kristensson**[1], **J. Löndahl**[1], **A. Eriksson**[1,2], **J. Pagels**[2], **and S. Gustafsson**[3]

[1]Division of Nuclear Physics, Lund University, 221 00, Lund, Sweden
[2]Division of Ergonomics and Aerosol Technology, Lund University, Sweden
[3]Environmental Department, City of Malmö, Sweden
[*]now at: National Environmental Research Institute, Dept. of Atmospheric Environment, Aarhus University, Denmark

Received: 14 July 2010 – Published in Atmos. Chem. Phys. Discuss.: 10 August 2010
Revised: 20 January 2011 – Accepted: 14 February 2011 – Published: 22 June 2011

Abstract. The climate effects downwind of an urban area resulting from gaseous and particulate emissions within the city are as yet inadequately quantified. The aim of this work was to estimate these effects for Malmö city in southern Sweden (population 280 000). The chemical and physical particle properties were simulated with a model for Aerosol Dynamics, gas phase CHEMistry and radiative transfer calculations (ADCHEM) following the trajectory movement from upwind of Malmö, through the urban background environment and finally tens and hundreds of kilometers downwind of Malmö. The model results were evaluated using measurements of the particle number size distribution and chemical composition. The total particle number concentration 50 km ($\sim$ 3 h) downwind, in the center of the Malmö plume, is about 3700 cm^{-3} of which the Malmö contribution is roughly 30%. Condensation of nitric acid, ammonium and to a smaller extent oxidized organic compounds formed from the emissions in Malmö increases the secondary aerosol formation with a maximum of 0.7–0.8 $\mu g\,m^{-3}$ 6 to 18 h downwind of Malmö. The secondary mass contribution dominates over the primary soot contribution from Malmö already 3 to 4 h downwind of the emission sources and contributes to an enhanced total surface direct or indirect aerosol shortwave radiative forcing in the center of the urban plume ranging from -0.3 to $-3.3\,W\,m^{-2}$ depending on the distance from Malmö, and the specific cloud properties.

1 Introduction

In recent years several studies have shown that anthropogenic emissions of trace gases and aerosol particles from urban areas are important for particle properties relevant for climate and population health, not only within the source region itself but also several hundred kilometers downwind (e.g. Seinfeld et al., 2004; Gaydos et al., 2007; Hodzic et al., 2009; Tie et al., 2009). Hence, there is an urgent need to accurately incorporate these urban emissions into regional and global three dimensional Chemistry Transport Models (3-D-CTMs) and even global climate models. The urban background stations measure freshly emitted particles in the beginning of the ageing process. Still, the distances from the emission sources are much shorter than the spatial scales used in global and regional CTMs (Pierce et al., 2009). Therefore, it is important to study the chemical and physical transformation of particles from urban background scale (0.1–1 km) to CTM grid scale (10–100 km scale). Several urban plume studies have been carried out within comprehensive but short field campaigns in large cities (>1 million people), e.g. Mexico City (Doran et al., 2007; Hodzic et al., 2009; Tsimpidi et al., 2010), Tampa (Nolte et al., 2008), Paris (Hodzic et al., 2006) and Copenhagen (Wang et al., 2010), while very few, if any, such studies have been carried out in small to midsize cities (<1 million people). Still, about 60% of the urban population of the world live in small to midsize cities (Population Div. of the Dep. of Economic and Social Affairs of the UN Secretariat), and by number they are far more common and well distributed over the globe than those who live in large cities. Even though one small city's emissions alone are of little concern on a global scale, they together cause a large portion of the global anthropogenic particle and gas phase emissions. Therefore it is important to consider these emissions when discussing climate and health effects of particles and gases on any spatial scale and to implement them into regional and global CTMs.

Most previous studies which have approached to model the ageing of urban particle and gas phase emissions downwind of urban areas have used Eulerian 3-D-CTMs with detailed gas and particle phase chemistry, but with relatively coarse spatial horizontal resolution (5×5 km – 36×36 km)

Correspondence to: P. Roldin
(pontus.roldin@nuclear.lu.se)

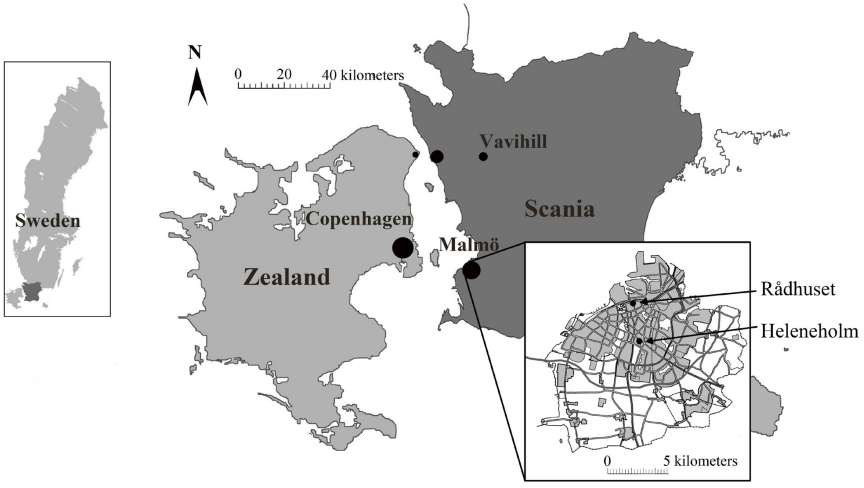

Fig. 1. Geographic map displaying the measurement station in Malmö (Rådhuset), the meteorological mast (Heleneholm) and the Vavihill field station in southern Sweden.

and only very few particle size bins (6–10) (e.g. Hodzic et al., 2006; Gaydos et al., 2007; Nolte et al., 2008; Hodzic et al., 2009). However, when implementing urban background emissions into CTMs, the spatial resolution should preferably be at least $1 \times 1\,\mathrm{km}^2$ and the size resolved chemical and physical properties relevant for climate and health effects are only poorly represented when using only a few size bins.

In this work a trajectory model for Aerosol Dynamics, gas phase CHEMistry and radiative transfer calculations (ADCHEM), developed at Lund University (Roldin et al., 2011), has been used to simulate the aging of the urban plume from the city of Malmö in Southern Sweden (13°00′ E, 55°36′ N, 280 000 people) during the year 2005 and 2006. ADCHEM includes all important aerosol dynamic processes, detailed gas and particle phase chemistry and dispersion in the vertical and horizontal direction, perpendicular to the urban plume. The computational advantage of the Lagrangian compared to the Eulerian approach allows the user to include a large number of size bins (in this study 100 size bins between 1.5 and 2500 nm in diameter) and still to keep a high horizontal and temporal resolution (in this study 1 km and 1 min). Hence, ADCHEM can be used to model the ageing of urban emissions from urban background to regional scales (several hundred kilometers from the source).

This work mainly describes the methods used to estimate the regional influence from the Malmö particle and gas phase emissions, the average results from these urban plume studies and finally gives estimates of different particle properties relevant for climate on the regional scale. For a detailed description and evaluation of ADCHEM the reader is referred to Roldin et al. (2011).

The aim of this study was to estimate the influence of the urban particle and gas phase emissions in Malmö on climate relevant particle properties downwind of the city, e.g. radiative forcing (ΔF). A second aim was to test methods and provide results that could form a basis for up-scaling from urban sub-grid emissions to the regional scale which can be treated by and implemented in regional and global 3-D-CTMs.

2 Methods for urban plume studies

In this section the methods used to characterize the properties of the aerosol particles inside the urban plume from Malmö is described. These methods were applied for 26 urban plume cases and the average and median results are presented in this article.

2.1 Measurements

Particle and gas phase concentration data from two different stations in Sweden were either used as input data in ADCHEM or to evaluate the model results. The stations were an urban background station positioned in Malmö (Rådhuset, 55°36′ N, 13°00′ E, 30 m a.s.l.) and the European Monitoring and Evaluation Program (EMEP) background station Vavihill (56°01′ N, 13°09′ E, 172 m a.s.l.), about 50 km north from Malmö (Fig. 1). A description of the measurement station Vavihill can be found in Kristensson et al. (2008).

The particle number size distributions in Malmö and Vavihill were measured with a Scanning Mobility Particle Sizer (SMPS) and a Twin Differential Mobility Particle Sizer (TDMPS), respectively. The SMPS system in Malmö measured the urban background particle number size distribution at the roof top level of the town hall (Rådhuset) in the north-western part downtown Malmö (Fig. 1). During southerly wind directions the station detected particle concentrations which are representative for the major particle emissions from Malmö.

The SMPS system in Malmö sampled air through a PM_{10} inlet (Patashnik and Rupprecht, 1991). The sampled particles were brought to charge equilibrium using a bipolar charger before size separation in a medium Vienna-type Differential Mobility Analyzer (DMA) (Winklmayr et al., 1991) and were subsequently counted by a Condensation Particle Counter (CPC) (model CPC 3760A) (TSI Inc., Shoreview, MN, USA). This way a full particle number size distribution between 10 and 660 nm in diameter was measured within 3 min. The short sampling time enabled the instrument to capture the rapidly changing particle concentrations at the urban site.

The TDMPS system at the Vavihill field station measured the rural background particle number size distribution from 3 to 900 nm with 10 min time resolution, in a similar way as the SMPS system in Malmö (Kristensson et al., 2008).

As an independent way of testing the accuracy of the ADCHEM model in describing the aerosol chemical composition, data from Time of Flight Aerosol Mass Spectrometry (ToF-AMS) measurements at Vavihill were compared with the average model results. The AMS measurements were not conducted at the time of the modeled period but during two campaigns in October 2008 and March 2009 (Eriksson, 2009). The AMS results (in total 40 h of data) are selected for periods with southerly originated air masses passing over the Malmö region between 1–6 h before they reach Vavihill. According to HYSPLIT model trajectories (Draxler and Rolph, 2011) these air masses have their origin from similar European source regions as the trajectories for the modeled case studies (e.g. Great Britain, Germany, Denmark, Benelux and Poland) (see Fig. 2). Because of the relatively few hours with AMS results for southerly originated air masses and the lack of AMS measurements at the time of the modeled period (April–November, 2005 and 2006), the model results cannot be directly compared with these measurements. The main reason for this is that meteorological conditions show both large diurnal and seasonal variations, which have a large influence on the gas to particle partitioning and formation rate of e.g. nitrate and condensable organic compounds. However, the AMS data still give a representative picture of the relative concentrations of different compounds in different size classes and hence, it is of great value for the evaluation of modeled chemical composition. Measured concentrations of NO, NO_2, O_3 and SO_2 at the urban background station in Malmö and in addition O_3 at Vavihill, from the modeled time periods, were compared with the modeled gas phase concentrations along the trajectory for each urban plume case. All gas concentrations were averaged to 1 h time resolution data when compared with the model results. NO_2 and NO_x were measured with chemiluminescence technique and SO_2 with UV-fluorescence technique. The total NO_x concentration is detected by first oxidizing all NO to NO_2. At both stations O_3 was measured using the principle of UV-absorption.

Apart from measured particle and gas phase concentrations, measurements of the wind direction from a meteorological mast in Malmö (Heleneholm) were used to verify that the urban plume from Malmö was directed towards Vavihill. The wind direction was measured at 24 m a.g.l. The position of the meteorological mast is displayed in Fig. 1.

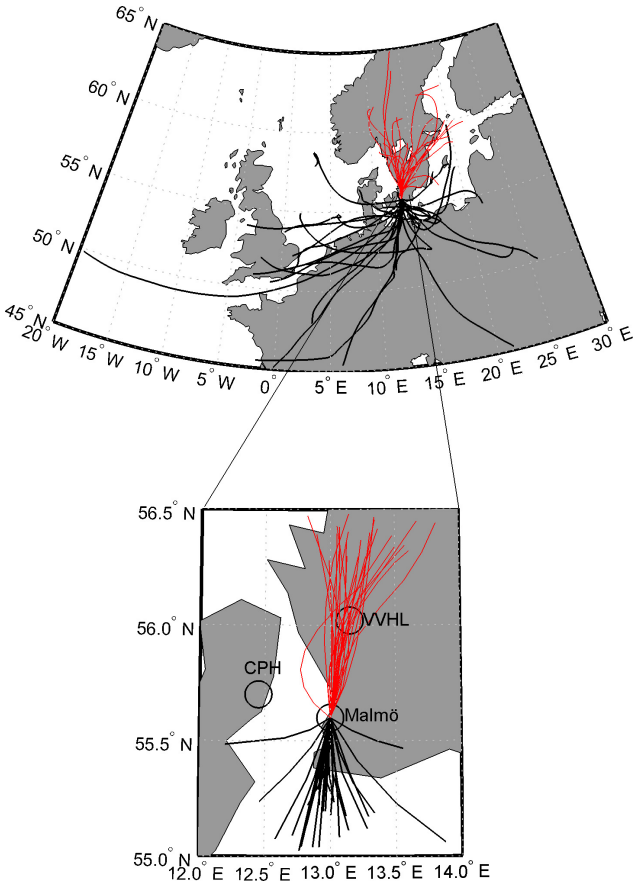

Fig. 2. 24 h forward trajectories (red) and 48 h backward trajectories (black) with starting point in Malmö for all the 26 urban plume cases. Vavihill (VVHL), Malmö and Copenhagen (CPH) are illustrated with circles.

2.2 The ADCHEM model

For more detailed information about all the modules and methods (e.g. condensation/evaporation algorithms, SOA formation models and size structure methods) and their influence on the model results the reader is referred to Roldin et al. (2011).

ADCHEM can be divided into three sub-models:

1. an atmospheric aerosol dynamics and particle chemistry model,
2. a chemical gas phase model,
3. a radiative transfer model.

The aerosol dynamic model is a sectional model which discretizes the particle number size distribution into finite size bins. The particles are assumed to be internally mixed which means that all particles of a certain size have equal composition. The model includes the following processes: condensation, evaporation, dry deposition, Brownian coagulation, wet deposition, in-cloud processing with dissolution of SO_2 and H_2O_2 forming sulfate (S(VI)), primary particle emissions, homogeneous nucleation and dispersion in the vertical (1-D model) and horizontal direction (2-D model) perpendicular to an air mass trajectory. The particle number size distribution changes upon condensation/evaporation and coagulation is either treated with the full-moving, full-stationary or moving-center structure method, which are all mass and number conserving (e.g. Jacobson, 2005b). The full-moving method is only useful for box-model simulations, because it cannot be used when particles are mixed between adjacent grid cells. In Roldin et al. (2011) it was shown that the moving-center structure method can give unrealistic size distributions if more than approximately 25 size bins between 1.5 and 2500 nm in diameter are used, while the full-stationary structure method gives significant numerical diffusion if less than 50 size bins are used. Because high size bin resolution was preferred, the full-stationary method with 100 size bins between 1.5 and 2500 nm in diameter was used for all simulations performed in this work.

The modeled aerosol particles are composed of sulfate, nitrate, ammonium, sodium, chloride, non water soluble minerals (metal oxides/hydroxides), soot, Primary Organic Aerosol (POA), Anthropogenic and Biogenic Secondary Organic Aerosol (ASOA and BSOA). With ADCHEM the SOA formation can either be modeled using the 2-product model approach (Odum et al., 1996), or using the 2-D-VBS method, which apart from saturation concentration (C^*) includes oxygen to carbon ratio (O/C-ratio) as a second dimension (Jimenez et al., 2009).

The condensation and evaporation of H_2SO_4, HNO_3, HCl and NH_3 can either be modeled as uncoupled or coupled processes (e.g. Zhang and Wexler, 2008). One advantage using the approach of coupled condensation is that the mass transfer of acids and bases becomes independent of pH in the particle water phase. The disadvantage is however that this method can only be used if the particles are near acid neutralized (S(VI) in the form of SO_4^{-2}) (Zaveri et al., 2008; Zhang and Wexler, 2008; Roldin et al., 2011). When using the approach of uncoupled condensation the condensation processes of acids and bases are treated as separate processes which depend on the pH in the particle water phase. Therefore this method can also be used when the aerosol particles are not fully acid neutralized. When considering uncoupled condensation ADCHEM uses the prediction of non-equilibrium growth (PNG) scheme developed by Jacobson (2005a). In this scheme the dissolution of ammonia is treated as an equilibrium process after the diffusion limited condensation/evaporation of all inorganic acids. This enables the model to take long time steps (minutes) without causing the modeled pH to start oscillating.

The gas phase model considers 130 different chemical reactions between 61 individual species. The majority of the reactions considered in the kinetic code was described by Pirjola and Kulmala (1998) but is originally from EMEP. Daily isoprene and monoterpene emissions were simulated separately with the vegetation model LPJ-GUESS (Smith et al., 2001; Sitch et al., 2003), in which process-based algorithms of terpenoid emissions were included (Arneth et al., 2007; Schurgers et al., 2009). These natural emissions were corrected for anthropogenic land cover according to Ramankutty et al. (2008).

In the present version of ADCHEM about one third of the non-methane volatile organic carbon (NMVOC) emissions from road traffic are benzene, toluene and xylene (BTX). These light aromatic compounds first react with OH followed by either reaction with NO forming products with low SOA-yields, or with HO_2 resulting in products with generally higher SOA-yields (Ng et al., 2007). In the supplementary material to Roldin et al. (2011) the benzene, toluene and xylene SOA yields from the 2-D-VBS model, for low and high NO_x conditions, are given as function of the total organic particle mass. At high NO_x/HO_2 ratios, which generally are the case in urban environments, most of the oxidation products will react with NO, while at remote regions and in the free troposphere the HO_2-pathway usually dominates. Hence, oxidation of BTX in urban environments generally gives relatively low SOA formation, while moving further away from the source the SOA formation can be considerably higher. Here it is mainly benzene, which is the least reactive of the three compounds, that is left to form SOA (Henze et al., 2008). In ADCHEM both the high and low NO_x reaction pathways are considered simultaneously. The reaction rate for the low-NO_x pathway is given by $k_{RO_2+HO_2} = 1.4\times10^{-12}\exp(700/T)\,\mathrm{cm^3\,molecule^{-1}\,s^{-1}}$ and the reaction rate for the high-NO_x pathway by $k_{RO_2+NO} = 2.6\times10^{-12}\exp(350/T)\,\mathrm{cm^3\,molecule^{-1}\,s^{-1}}$ (the Master Chemical Mechanism v 3.1 (http://www.chem.leeds.ac.uk/Atmospheric/MCM/mcmproj.html)).

The radiative transfer model is used to derive the spectral actinic flux which affects the photochemical reaction rates. This model uses a quadrature two-stream approximation scheme, where the radiative fluxes are approximated with one upward and one downward flux component. This scheme was developed and used by Toon et al. (1989) to calculate the radiative transfer in a vertically inhomogeneous atmosphere with clouds and aerosol particles.

In Roldin et al. (2011) it was illustrated that the particles in the urban plume from Malmö are at least not always completely acid neutralized. Hence, for all simulation performed in this work the condensation of acids and bases were treated as uncoupled processes. The SOA formation was modeled with 2-D-VBS for high and low NO_x conditions according to the parameterization in Roldin et al. (2011). The POA

was modeled as semi-volatile (with a C^* between 10^{-2} and $10^4\,\mu g\,m^{-3}$) and the intermediate VOC (IVOC) emissions (C^* between 10^4 and $10^6\,\mu g\,m^{-3}$) was assumed to be 1.5 times larger than the anthropogenic POA emissions according to Robinson et al. (2007). The volatility of the POA emissions and the IVOC emissions are uncertain, but these values have been used as best estimates in several previous model studies (e.g. Robinson et al., 2007; Shrivastava et al., 2008; Tsimpidi et al., 2010). For all simulations performed in this work the POA emissions were initially treated as entirely in the particle phase. However, downwind of the emission source most of this organic material evaporates from the particles. In the gas phase this material is oxidized and then again returns to the particle phase as oxidized organic compounds. In Roldin et al. (2011) several sensitivity tests were performed with ADCHEM to study the effect of SVPOA or non-volatile POA and the importance of the IVOC emissions.

The 2-D-VBS model in ADCHEM considers the kinetic (diffusion limited) condensation/evaporation of 110 different organic compounds, separated into 10 different volatility classes with C^* between 10^{-2} and $10^7\,\mu g\,m^{-3}$ and 11 different O:C-ratio levels from 0 to 1. One large assumption with the 2-D-VBS is that the gas phase compounds, independent of their origin, react with OH with the same reaction rate, equal to $3 \times 10^{-11}\,cm^3\,molecule^{-1}$ (Jimenez et al., 2009). The reaction rates for the first oxidation step of all monoterpenes, isoprene, benzene, toluene and xylene, are however species specific and considered before the formed oxidation products enter the VBS. The only compounds which enter directly into the VBS before they have been oxidized are POA species and IVOCs. For each oxidation reaction in the 2-D-VBS, one to three oxygen atoms are added to the oxidized molecule according to a probability distribution function. The formed oxidation product can then either stay intact (functionalize) or fragmentize into several smaller molecules. Depending on the size of the fragments and the number of added oxygen atoms, they can either have lower or higher volatility than the original molecule. However, if the oxidation product is not fragmentized it will always have lower volatility than the original molecule (see Roldin et al., 2011 for details).

The 2-D-VBS model gives a particle size dependent partitioning of the different condensable organic compounds, with larger fraction of low volatile compounds found in the smaller particle sizes and a larger fraction of more volatile compounds found in the larger particle sizes. The kinetic and particle size dependent condensation/evaporation processes require that ADCHEM keeps track of all the different organic compounds in each particle size bin, which is computationally expensive, especially for the coagulation algorithm (for more information see Roldin et al., 2011).

2.3 Model inputs

Meteorological data from the Global Data Assimilation System (GDAS) were downloaded from NOAA Air Resource Laboratory Real-time Environmental Application and Display sYstem (READY) (Rolph, 2011). Along each trajectory, data of solar irradiance, mixing height and rainfall intensity with one hour time resolution was included. For every three hours along the trajectories, vertical temperature and relative humidity profiles were received. The vertical temperature and relative humidity data was linearly interpolated to the fixed vertical grid that was used for the simulations. Linear interpolation of all meteorological data was also carried out to increase the temporal resolution to 1 min, which was the time step used by ADCHEM.

Country specific forest and meadow/pasture area coverage information from Simpson et al. (1999), and emissions of isoprene and monoterpenes from LPJ-GUESS and anthropogenic NMVOCs, NO_x, SO_2, CO, NH_3 and $PM_{2.5}$ emissions were included along the trajectories. For Denmark and southern Sweden (54°48′ N to 56°22′ N) the anthropogenic yearly average emissions along the trajectories were received from the National Environmental Research Institute (NERI) in Denmark and the Environmental Dept., City of Malmö (Gustafsson, 2001) in Sweden, respectively. For Danish road emissions, a spatial resolution of $1 \times 1\,km^2$ was obtained, based on NERI's traffic database with traffic volumes on all road links in Denmark for the year 2005, together with emission factors from the COPERT IV model applied for 2008. For other (non-road) sources in Denmark, an emission inventory with $17 \times 17\,km^2$ spatial resolution was used based on Danish national emission inventories for the year 2007 provided by NERI (http://emission.dmu.dk). For southern Sweden, all anthropogenic emissions had a spatial resolution of $1 \times 1\,km^2$. The southern Swedish emission data base has previously primary been used for epidemiological studies in relation to NO_x and NO_2 exposure (e.g. Chaix et al., 2006; Stroh et al., 2007). For the rest of Europe the emissions within our study were taken from the EMEP emission database for year 2006 (Vestreng et al., 2006). These emissions have a spatial resolution of $50 \times 50\,km^2$. The yearly anthropogenic emissions were multiplied with country specific diurnal, weekly and monthly variation factors based on the EMEP emission database. The forest and meadow/pasture data was used to estimate the surface albedo and roughness length.

The measured particle number size distributions were averaged to 30 min values in Malmö and at Vavihill. They were parameterized by fitting 5 modal lognormal distributions to the data using the automatic lognormal fitting algorithm DOFIT, version 4.20 (Hussein et al., 2005). Because of the lower detection limit of 10 nm for the SMPS system in Malmö, the actual number concentration of the nucleation mode particles in Malmö is uncertain. The particle number size distributions upwind of Malmö were estimated from the measured

background conditions at Vavihill (see Sect. 2.4) and used as initial condition in the model. Limitations and uncertainties with this method are discussed in Sect. 2.7. The contribution from local emissions in Malmö was derived as the difference between the estimated background size distribution and the measured size distribution in Malmö. These particles mainly originate from road traffic within the city. In Sect. 2.5 a description is given of how these local particle emissions were introduced into the model over Malmö.

The initial (48 h upwind of Malmö) $PM_{2.5}$ chemical composition was estimated from the aerosol mass spectrometer (AMS) measurements carried out at several European sites (Jimenez et al., 2009) with approximately 35% organic matter, 26% sulfate, 7% nitrate, 12% ammonium, 3% soot and 17% minerals (metal oxides/hydroxides) below 1000 m a.g.l. and changing linearly to the top of the model domain (2000 m a.g.l.) to 23% organic matter, 36% sulfate, 11% nitrate, 17% ammonium, 2% soot and 11% minerals.

2.4 Background particle properties outside the urban plume

To be able to estimate the contribution of urban emissions to the regional background particle concentration between Malmö and Vavihill, the background without influence of the urban plume has to be approximated. This was achieved by selecting measured particle number size distributions averaged to 30 min values before and after the time of arrival of the urban plume from Malmö, at Vavihill. The background was estimated as the average of these two 30 min averages. This background particle number size distribution was also used to represent the conditions upwind of Malmö (see Sect. 2.7). The detailed criteria for the selection of background distributions are:

1. The trajectories should not move over Malmö or Copenhagen before they reach Vavihill.
2. At the time for the measurement of the estimated background, the air mass trajectory reaching Vavihill should originate from the same source region, 48 h backward in time, as the trajectory influenced by the Malmö plume.
3. The selected background particle number size distribution should have been measured within 6 h before or after the urban plume reached Vavihill.
4. The selected background particle number size distributions before and after the Malmö plume observed at Vavihill should have similar shape and magnitude.
5. The original particle number size distribution at 10 min time resolution should show only low temporal variability within the averaging period.
6. If several particle number size distributions seemed to obey criteria 1 to 5 equally well, the distribution measured nearest in time before or after the Malmö plume reached Vavihill was selected.

2.5 Spin-up time upwind of Malmö

The total run time of each simulation was three days, starting two days before the air mass trajectory reached Malmö and continuing one day downwind of Malmö. The first two days of the simulations were used to initialize (equilibrate) the particle and gas phase chemistry. During this time the particle number size distribution was kept fixed, while all other parameters were allowed to change. After the trajectory reached the urban background station in Malmö, the particle number size distribution was also allowed to change.

When the trajectory arrived at the southern border of Malmö, the estimated size dependent local particle number concentration contribution was included in each grid cell within the boundary layer, according to Eqs. (1) and (2). With these equations the particle emissions are scaled horizontally using the accumulated horizontal (west to east) NO_x-emission profile (E_{NO_x}) from the southern border of Malmö to the measurement station. Equation (1) gives the estimated particle number concentration in each diameter size bin at the time when the trajectory arrived at the measurement station in Malmö, while Eq. (2) gives the estimated particle number concentration in each diameter size bin for each time step (i) between the southern border of Malmö ($i = 1$) and the measurement station ($i = N$), at the north western part of the city. Equation (2) takes into account the dynamic and chemical processing of the aerosol number size distribution in each time step between the southern border and the measurement station in the northern part of Malmö. Hence, it is not just a simple linear interpolation of the particle number size distribution between these two points ($i = 1$ and $i = N$). Instead it is a linear interpolation for each time step, but of a different kind that includes the effects of dynamic and chemical processing on the particle number size distribution in the previous time step. In other words, for each of the time steps (i), the interpolation is performed between the concentration one time step backwards ($i-1$) from the current time step and the final time step at the measurement station (time step N).

$$c_N^j(D_p) = c_{backg}(D_p) + \frac{\sum_{k=1}^{N} E_{NO_x}^j}{\sum_{k=1}^{N} E_{NO_x}^{center}} c_{traffic}(D_p) \quad (1)$$

$$c_i^j(D_p) = \left(\frac{N-i}{N} c_{i-1}^j(D_p) + \frac{i}{N} c_N^j(D_p)\right) \quad (2)$$

$c(D_p)$ in Eqs. (1) and (2) is the concentration of particles with a diameter equal to D_p. N is the number of time steps which the trajectory travels over Malmö before reaching the measurement station. c_{backg} (D_p) is the estimated background

particle number concentration outside Malmö (initial concentration), j is the horizontal grid cell index (1–20), $E^{j}_{NO_x}$ is the NO_x emissions factor from road traffic at the horizontal grid cell index j, $E^{center}_{NO_x}$ is the NO_x emission factor from road traffic in the center of the horizontal model domain ($j = 10$ and 11) and i is the time step index which starts at 1 when the air mass reaches the southern border of Malmö and reaches N, when the trajectory arrives at the measurement station. $c_{traffic}(D_p)$ is the estimated size-dependent local particle number concentration contribution from road traffic in the center of the urban plume, which was derived by taking the difference between the measured particle number size distribution in Malmö and the estimated upwind background particle number size distribution (Sect. 2.4). When using Eq. (1) the particle number size distribution at the center of the urban plume within the boundary layer becomes comparable to the measured particle number size distribution in Malmö at that time. The horizontal (west to east) NO_x emission profile (E_{NO_x}) for Malmö was derived from the NO_x emission database from road traffic within Malmö by averaging the horizontal NO_x emission profiles at the western and eastern side of the trajectory, upwind of the measurement station. The NO_x emission profile resembles a Gaussian distribution with a maximum in the center of the urban plume ($E^{center}_{NO_x}$) and with a full width at half maximum of 7 km. Since the NO_x emissions from road traffic in Malmö are largest in the center of the horizontal model domain, the particle concentrations derived in the model are highest at the measurement station and drop towards the estimated background concentrations at the horizontal boundaries.

2.6 When does the urban plume from Malmö influence Vavihill?

Wind direction measurements from the meteorological mast in Malmö together with HYSPLIT trajectories were used for a first selection of days with possible influence from Malmö on the background station Vavihill. In total 39 days were identified between April 2005 and October 2006. From these days 232 case studies were selected to cover all periods with possible influence from Malmö on Vavihill. All these cases were then modeled using a simplified 1-D version of ADCHEM, excluding detailed particle and gas phase chemistry and homogeneous nucleation, and assuming a fixed concentration of 10^7 molecules cm^{-3} of a non-volatile condensable compound with a molar mass of 150 g mol^{-1}. The modeled particle number size distributions at Vavihill were compared with the measured particle number size distributions at Vavihill at the time of arrival of the trajectories. For cases with less than 20% difference between the measured and modeled number and surface area concentration, and less than 30% difference in the volume concentration between 10 and 600 nm in diameter, it was considered to be likely that the Malmö emissions influenced Vavihill. In total, 67 out of 232 cases, from 26 out of 39 days fulfilled these criteria.

Table 1. Diurnal, weekly and monthly distribution of all 26 simulated cases. The time is given as local wintertime at the time when the trajectories arrived in Malmö.

Day	Mon.	Tue.	Wed.	Thu.	Fri.	Sat.	Sun.
No. of sim.	6	2	1	6	1	5	5
Month	Apr.	May	Jun.	Jul.	Aug.	Sep.	Oct.
No. of sim.	1	4	8	3	0	3	7
Time	00:00–06:00	06:00–12:00		12:00–18:00		18:00–00:00	
No. of sim.	7	7		7		5	

Cases with rainfall between Malmö and Vavihill were not considered. However, for several cases rainfall was occurring both upwind of Malmö and downwind of Vavihill. The 67 cases were then modeled with a complex 1-D version of ADCHEM, which included all processes considered by the model except horizontal dispersion. From these simulations, the case with best agreement between the model and measurements, from each of the 26 days was finally selected. Only one case was selected for each day to ensure that certain conditions were not overrepresented, when deriving the average properties of the urban plume. For all of these 26 cases the modeled and measured number and surface area concentration agreed within 10% and the volume concentration within 20% for particles between 10 and 600 nm in diameter. Table 1 gives the diurnal, weekly and monthly distribution of all 26 case studies. Due to a lack of parallel measurements at Vavihill and Malmö station, no urban plume studies for the period November to March could be carried out.

2.7 The upwind background particle number size distributions

The background contribution to the particle number size distribution in Malmö and upwind of Malmö was approximated with the measured Vavihill background size distribution as described in Sect. 2.4. This relies on the premise that the particle number size distribution for the background is not changing between upwind of Malmö and Vavihill which is a distance of about 50 km. However, the distributions are not identical at these sites in reality due to aerosol dynamic processes. To illustrate this, the modeled background particle number size distribution outside the urban plume at Vavihill can be compared with the estimated upwind of Malmö particle number size distribution (measured Vavihill background particle number size distribution) (see Fig. S1 in the online supplementary material). Figure S1 shows that the particle number size distribution is altered during the air mass transport between upwind of Malmö and Vavihill for the average of the 26 model cases described in Sect. 2.6. On the other hand, the second message from this exercise is that this change is relatively small (about 200 cm^{-3} or 8% lower

particle number concentration between 5 and 1000 nm, outside the urban plume at Vavihill compared with upwind of Malmö), and hence can be considered acceptable for the model experiments.

2.8 Estimating the secondary aerosol formation within the urban plume

All 26 selected case studies were modeled with and without anthropogenic gas phase emissions in Malmö. The anthropogenic gases considered were NO_x, SO_2, CO, NMVOCs, and the IVOCs. All other conditions for the simulations except the emissions of these gases in Malmö were identical for the two model setups. The difference between the results with or without anthropogenic gas phase emissions in Malmö were then used to estimate the importance of these emissions for the secondary aerosol formation and to answer the question of how this secondary aerosol formation influences the climate relevant particle properties downwind of the city.

2.9 Climate relevant particle properties downwind of Malmö

Using the modeled average particle properties within the urban plume downwind of Malmö, attempts were made to estimate the shortwave radiative forcing (ΔF) of Malmö emissions on the regional scale, with and without clouds. The radiative forcing due to the gas phase and particle emissions in Malmö was calculated for different distances (or hours) downwind of Malmö.

To be able to estimate the yearly average shortwave radiative forcing from the Malmö emissions, the average particle properties for the 26 case studies were assumed to be representative for the yearly average particle properties in the Malmö urban plume within the boundary layer. From October to March the boundary layer height was assumed to be 300 m during the night reaching a maximum of 500 m during the day, while between April and September it was assumed to be 300 m during the night reaching a maximum of 1200 m during the day. For the investigation of light scattering and absorption of the aerosol particles, the average relative humidity profile from all 26 simulations in Malmö was used, with an average relative humidity of 78% within the lowest 2000 m of the atmosphere. The particle growth factors due to water uptake were calculated with the thermodynamic model used in ADCHEM. Size-resolved refractive indices of the aerosol particles were estimated from the modeled volume fractions of soot, organic matter, minerals (metal oxides/hydroxides), water soluble inorganic salts and water, with refractive indices reported by Schmid et al. (2009), Horvath (1998) and Sokolik and Toon (1999).

The radiative forcing at the surface and at the top of the atmosphere (TOA) caused by the emissions in Malmö was calculated by taking the difference between the modeled irradiance inside and outside the urban plume. The shortwave radiative forcing of the Malmö particle emissions was calculated for each hour of the day (24 h) of each month of the year and then averaged to get the estimated yearly average shortwave radiative forcing in the urban plume from Malmö.

To be able to estimate the radiative forcing during the presence of clouds an adiabatic cloud parcel model was used to derive realistic cloud properties (Jacobson, 2005b). Although they are realistic, these cloud properties are only hypothetical and will not be fully representative of the yearly average cloud cover in the Malmö region. Therefore, the derived shortwave radiative forcing during the presence of clouds should not be considered as the best estimate of the yearly average shortwave radiative forcing from the Malmö emissions. The calculations are instead intended to illustrate that the shortwave radiative forcing of the gas and particle emissions can be substantially different during completely cloudy and non-cloudy days.

The adiabatic cloud parcel model calculates the relative humidity, temperature, total liquid water content (LWC), particle number and cloud droplet number size distributions, as a function of the altitude of an air parcel with a pre-specified updraft velocity, taking into account the adiabatic expansion and the latent heat release upon condensation. Raoult's law and the Kelvin effect are used to derive the water saturation concentration in moles per cubic centimeter of air above each particle or droplet surface, and then the concentration gradient between the gas and particle phase, which drives the mass transfer to or from the particle surfaces, is updated for each time step. For a more detailed description of the model, the reader is referred to Jacobson (2005b).

According to Rogers and Yau (1989) typical updraft velocities for stratus clouds are on the order of a few tens of centimeters per second and for cumulus clouds in the order of meters per second. For the simulations performed in this work the updraft velocity inside the clouds was assumed to be 1.0 m s^{-1}. The mass accommodation of the condensing water as well as the thermal accommodation coefficient used to calculate the thermal conductivity of the latent heat release of evaporating water were set equal to one. The number of size bins was set to 200 between 50 nm and 1000 nm in dry particle diameter. The chemical and physical particle properties from ADCHEM were linearly interpolated to fit the diameter size resolution. Only the inorganic salts were allowed to take up water, while the organic fraction was treated together with minerals and soot as an insoluble core. The condensation/evaporation solver used the full moving structure method to account for the changing particle sizes (see e.g. Jacobson, 2005b or Roldin et al., 2011).

In the radiative transfer model 100 m or 500 m thick clouds with properties modeled with the adiabatic cloud parcel model were included at the top of the boundary layer. The absorption of infrared radiation inside the clouds was not considered in the model.

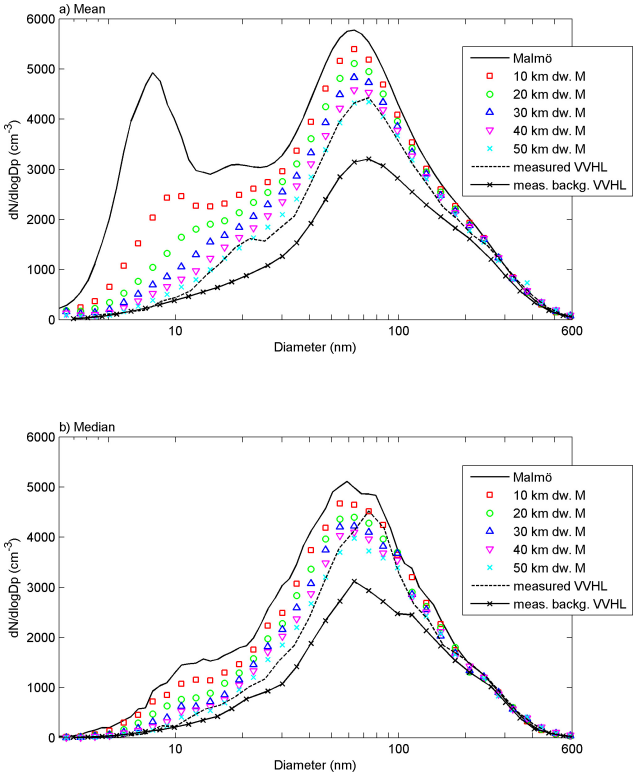

Fig. 3. Modeled average **(a)** and median **(b)** particle number size distributions in the center of the urban plume, 10, 20, 30, 40 and 50 km downwind of Malmö, together with the measured particle number size distributions in Malmö and at Vavihill (50 km downwind of Malmö). The displayed size distributions in Malmö were derived from the SMPS measurements applying the lognormal fitting algorithm from Hussein et al. (2005) for each individual size distribution and then taking the average and median of these size distributions.

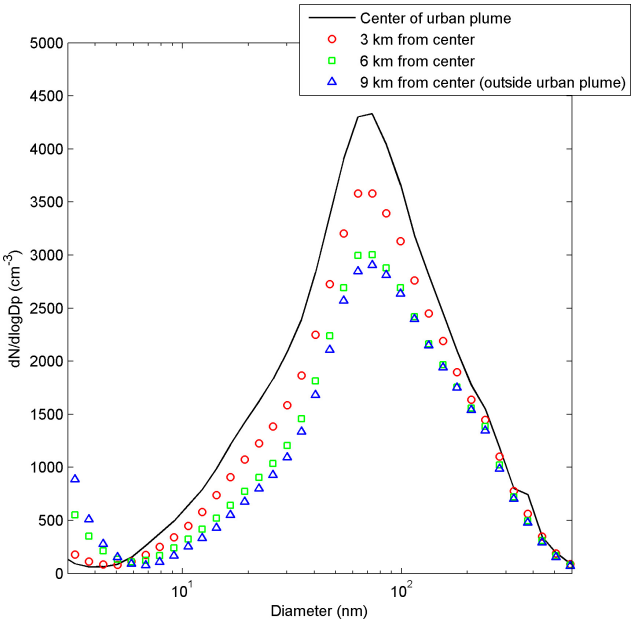

Fig. 4. Modeled average particle number size distributions at different distances (perpendicular to the air mass trajectories) from the center of the urban plume at Vavihill.

3 Results and discussion

The influence of Malmö city emissions on rural background particle concentrations is studied in 26 different cases using HYSPLIT air mass trajectories starting upwind of Malmö, going over Malmö and stretching hundreds of kilometers downwind of Malmö (Fig. 2). Most of the simulated trajectories originate over continental Europe (e.g. Germany, Poland and Benelux) or Great Britain. The trajectories pass over the EMEP background station Vavihill, ca 50 km downwind and north of Malmö. Vavihill is used for the validation of aerosol properties modeled with ADCHEM. Downwind of Vavihill, the majority of trajectories continue northward over Sweden.

3.1 Modeled and measured particle number size distributions in the urban plume of Malmö

Figure 3 illustrates the modeled average (a) and median (b) particle number size distributions in Malmö and at different distances downwind of Malmö in the center of the urban plume. As a comparison the measured average and median particle number size distributions at Vavihill, with or without influence from Malmö are also displayed. The shape of the size distribution 50 km downwind of Malmö from modeling and from measurements at Vavihill is identical in the urban plume and the total number concentration agrees to within 3% and 0.2% for the average and median, respectively. This indicates that the modeled particle number size distributions in the urban plume between Malmö and Vavihill are realistic. The relatively large concentration ($\sim 2000\,\mathrm{cm}^{-3}$) in the nucleation mode for the average particle number size distribution in Malmö is due to two daytime cases when the nucleation mode in Malmö was clearly dominating the total number concentration. These particles have a relatively short lifetime (minutes to hours) because of coagulation and dry deposition processes downwind of Malmö. However, a fraction ($\sim 30\%$) of these particles survives in the atmosphere all the way to Vavihill, where they appear as a mode around 18 nm in diameter. The lognormal parameterizations of the modeled particle number size distributions in Fig. 3a and b, derived with the DO-FIT algorithm, are given in Table S1 and S2 in the online supplementary material.

Figure 4 shows the modeled average particle number size distributions at the time of arrival at Vavihill at different distances from the center of the urban plume (perpendicular to the air mass trajectory). The results illustrate that for a compact and homogeneously populated city like Malmö the urban influence on the particle properties 50 km downwind of the city often decreases steeply from the urban plume center

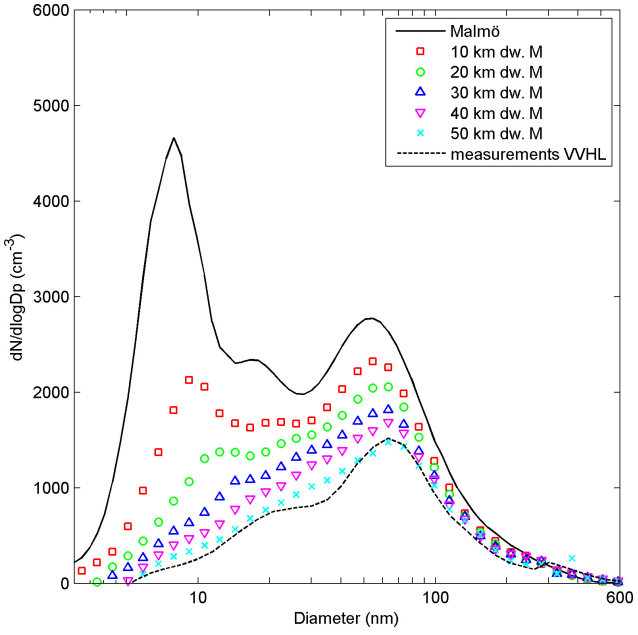

Fig. 5. Estimated average local emission contribution from Malmö, in Malmö, 10, 20, 30, 40 and 50 km downwind of the city. The particle number size distributions were derived by subtracting the modeled background particle number size distribution from the modeled particle number size distributions in the center of the urban plume, at different distances downwind of Malmö. The result from Vavihill was derived by subtracting the measured particle number size distribution at Vavihill when the station was not influenced by the Malmö plume from the measured particle number size distribution at Vavihill when the station was influenced by the Malmö plume.

towards the urban plume boundaries with only marginal influence more than 6 km outside the center of the urban plume.

By subtracting the modeled background particle number size distribution outside the urban plume (9 km from the center of the urban plume) from the modeled distributions inside the plume, the urban emission contribution in the center of the urban plume was estimated at different distances downwind of Malmö (see Fig. 5). As a validation of the model results the urban contribution at Vavihill (50 km downwind of Malmö) was also derived directly from the measured particle number size distributions inside and outside the urban plume. Within Malmö city and close to Malmö the emissions have a large influence on the nucleation and Aitken mode particle concentration. However, most of the nucleation mode particles formed in Malmö are lost by coagulation and dry deposition before the urban plume reaches Vavihill. The soot mode particles mostly originated from traffic, indicated at about 50 nm in Malmö, grew because of condensation to about 65 nm, 50 km downwind of the city. As will be shown in Sect. 3.4 this condensational growth is important for these particles' ability to form cloud droplets.

Table 2 gives the average and median total particle number, surface area and volume concentration (PN_{tot}, PA_{tot} and PV_{tot}) and average and median corresponding urban contribution (ΔPN_{urban}, ΔPA_{urban} and ΔPV_{urban}) for particles between 5 and 1000 nm in diameter at different distances downwind of Malmö. The urban contribution was derived by taking the difference between the concentration in the center of the urban plume and outside the urban plume (background). The total particle number concentration decreases rapidly downwind of Malmö, mainly due to coagulation of the freshly emitted particles onto the long distance transported accumulation mode particles. The estimated Malmö city average contribution to the urban background number concentrations is 58% or 3825 cm^{-3} in absolute terms. At Vavihill, 50 km downwind of Malmö, the average Malmö number concentration contribution is 34% (1291 cm^{-3}) according to the model and 32% (1177 cm^{-3}) according to the DMPS measurements. The modeled volume concentration contribution from the emissions in Malmö increases with 28% between Malmö and 50 km downwind of the city center (from 1.49 to 1.9 $\mu m^3\ m^{-3}$), mainly attributed to the secondary aerosol formation within the urban plume. The last two rows in Table 2 give the estimated average and median number, surface area and volume concentration contribution at Vavihill, derived from the particle number size distribution measurements. The number concentration contribution derived from the model at Vavihill is 10% higher for the average and less than 1% lower for the median concentration contribution compared to the measurements. For the surface area and volume concentration contribution the model gives 3% and 2% higher average and 3% lower and 23% higher median values compared to the measurements at Vavihill, respectively.

Table 2. Estimated average and median particle number, surface area and volume concentration (PN_{tot}, PA_{tot}, and PV_{tot} respectively) and its contribution from Malmö (difference between the center of the urban plume and the background) (ΔPN_{urban}, ΔPA_{urban}, and ΔPV_{urban}) for particles between 5 and 1000 nm in diameter in the center of the urban plume, at different distances downwind of Malmö (dw. M.).

Location	$PN_{tot}/\Delta PN_{urban}$ (cm^{-3})	$PA_{tot}/\Delta PA_{urban}$ ($\mu m^2\ cm^{-3}$)	$PV_{tot}/\Delta PV_{urban}$ ($\mu m^3\ m^{-3}$)
Malmö mean	6577/3825	204.1/48.1	8.28/1.49
Malmö median	4459/2049	151.8/30.2	5.53/0.75
10 km dw. M. mean	5313/2587	198.8/43.3	8.25/1.48
10 km dw. M. median	4001/1619	146.7/26.0	5.47/0.74
20 km dw. M. mean	4728/2082	197.6/41.2	8.38/1.46
20 km dw. M. median	3707/1416	146.0/26.6	5.60/0.82
30 km dw. M. mean	4325/1734	197.5/41.2	8.57/1.61
30 km dw. M. median	3486/1235	147.8/29.0	5.86/1.07
40 km dw. M. mean	4029/1520	198.5/43.1	8.82/1.82
40 km dw. M. median	3311/1117	147.7/27.9	6.00/1.11
50 km dw. M. mean	3763/1291	198.3/42.2	9.02/1.90
50 km dw. M. median	3128/960	143.9/23.1	5.86/0.86
VVHL mean	3648/1177*	197.0/40.8*	8.98/1.86*
VVHL median	3135/968*	144.5/23.7*	5.70/0.70*

* Derived from the DMPS measurements at Vavihill.

3.2 Uncertainties with the urban emission contribution downwind of Malmö

There are several reasons why the modeled and measured urban concentration contributions are uncertain. Listed are the two reasons which are regarded as the most important.

1. The method used to estimate the urban contribution downwind of Malmö requires that the measured background particle number size distribution at Vavihill is representative for the background conditions outside the urban plume between Malmö and Vavihill. The criteria for the selection of the background distributions were therefore designed to fulfill this requirement (see Sect. 2.4). However, since the background distributions at the time of arrival of the urban plume have to be approximated from the measurements a few hours before and after the urban plume influences Vavihill, some uncertainties with the derived background distributions still remain. Also instrumental errors influence the size distribution. In an intercomparison workshop at the Leibniz Institute for Tropospheric Research in Leipzig, Germany (Wiedensohler, et al., 2010), different SMPS/DMPS systems agreed within $\pm 10\%$ for a simulated size distribution in the size range from 20 to 200 nm in diameter. In reality, the total concentration spans over several magnitudes, the size range below 20 nm increases the error margin, and the instrument control and maintenance is not as thoroughly supervised as under laboratory conditions. The uncertainty of the choice of the background size distribution and the instrumental uncertainties should add up to a total uncertainty a few percent higher than the $\pm 10\%$ uncertainty estimated at the workshop. In order not to underestimate the uncertainty, a conservative value of 20% was chosen as the total uncertainty. A 20% error in the estimated average background number concentration outside Malmö would cause an error in the estimated urban contribution within the city of only 13%. However, at Vavihill, where the difference between the background and urban plume number concentration is smaller, the error would become 38%.

2. Another difficulty is the selection of the periods when the urban plume from Malmö affects the background station. In this work, wind direction measurements, HYSPLIT air mass trajectories and aerosol dynamics model simulations were used to find out when the plume from Malmö influenced the background station at Vavihill. On the one hand, these methods are objective in the sense that they do not introduce any bias in terms of individual opinions on how the size distribution downwind of the city "should" look like. On the other hand, these methods are an uncertain way to trace the anthropogenic influence. For better precision, the methods could be complemented with measurements of NO_x or CO at the background station, which could be used as tracers for the urban influence. Unfortunately, these measurements were not available from the station at Vavihill for time periods when this study was carried out.

Other processes with large model uncertainties but with only small to moderate influence of the urban contribution within 50 km downwind of Malmö are:

1. The homogeneous nucleation rate and initial growth rate of the smallest particles.

2. The primary particle emissions downwind of Malmö.

3. The gaseous emissions both upwind and downwind of Malmö and the corresponding SOA formation.

For none of the 26 days which were modeled, significant new particle formation was observed for several consecutive hours at both measurement stations. This indicates that for none of these days large scale regional nucleation events were occurring. Hence, the new particle formation between Malmö and Vavihill was likely also moderate or insignificant for these days, indicated by the good agreement between the model results and the measurements at Vavihill. For 2 out of 26 days large numbers of particles were however observed in the nucleation mode at the measurement station in Malmö. These particles were likely formed from local sources in or near Malmö (e.g. ship traffic). Even though none of the 26 selected days was characterized by large scale nucleation events, homogeneous nucleation can possibly have biased the average results presented in this study. The reason for this is that the simplified model used to make a first selection of possible days with influence from Malmö at Vavihill did not consider homogeneous nucleation and therefore systematically filtered out days with large new particle formation between Malmö and Vavihill.

Although the primary particle emissions downwind of Malmö are uncertain, only marginal effects are expected because of this uncertainty between Malmö and Vavihill. However, the effect might become much larger up to 24 h downwind of Malmö, both for the particle concentrations and chemical composition.

The gaseous emissions both upwind and downwind of Malmö are also uncertain (especially for the IVOCs), which affects the precision of secondary aerosol formation. Finally, most of the reactions involved in the secondary organic aerosol formation are unknown, which gives high uncertainty for this process. Most of these reactions are believed to be too slow to form large amount of SOA between Malmö and Vavihill. However, as for the other processes the uncertainties increase significantly with the distance downwind of Malmö.

Table 3. Measured and modeled average gas phase concentrations in Malmö and at Vavihill for the 26 model cases.

Species and location	Measured average (ppb)	Modeled average (ppb)
O_3 Malmö	25.7	31.5
O_3 Vavihill	32.4	34.3
NO Malmö	2.8	3.5
NO_2 Malmö	11.2	9.5
SO_2 Malmö	1.1	1.1

3.3 Modeled and measured particle and gas phase chemistry

A reasonable agreement between the modeled and the measured gas phase concentrations is important for the modeled particle chemistry. Although the deviation for certain gas phase species is higher than 100% for single case studies, the agreement is better between the average modeled and the measured concentrations as shown in Table 3.

The modeled average ozone concentration in Malmö is about 20% higher than the measured average value, while at Vavihill the model is less than 6% higher than the measurements. Both the measurements and the model give considerably lower ozone levels in Malmö than at Vavihill, with larger differences for the measurements compared to the modeled values.

For NO and NO_2 the modeled concentrations deviate with about 25% and −20% compared to the measured concentrations, respectively. However, the modeled NO_x ($NO + NO_2$) concentration is only 7% lower than the measurements. In the model the molecular NO/NO_x emission ratio was set to 0.9 for all NO_x emission sources. This ratio should probably be lower for better agreement between the modeled and the measured NO and NO_2 concentrations in Malmö. The modeled average SO_2 concentration in the surface layer is identical to the measured concentration.

Figure 6 displays the modeled average $PM_{2.5}$ mass fractions of all chemical compounds considered by the model from 6 h upwind of Malmö until 24 h downwind of Malmö. At Malmö the soot, organic matter and mineral (metal oxides/hydroxides) mass concentrations increase because of the primary particle emissions in the city. According to the model the total organic particle content makes up between 25% and 33% of the total $PM_{2.5}$ mass, with a minimum about 15 h downwind of Malmö. In Malmö 28% of the total organic $PM_{2.5}$ mass is composed of non-oxidized organic material (O:C-ratio equal to zero). This non-oxidized organic material decreases continuously and comprises only 22% of the total organic $PM_{2.5}$ mass 24 h downwind of Malmö. The only sources for these non-oxidized compounds in the 2-D-VBS are low volatile POA emissions which stay in the particle phase upon dilution in the atmosphere. The inorganic salt content is dominated by ammonium nitrate, with a nitrate $PM_{2.5}$ mass fraction varying between a minimum of 24% in Malmö to a maximum of 36% 15 h downwind of Malmö. As expected, the ammonium concentrations show a clear correlation with the nitrate content. According to the model the PM in the urban plume is fully or partly neutralized, with an average of between 1.86 and 1.74 ammonium ions available to neutralize each sulfate ion. The particles were least neutralized 24 h downwind of Malmö.

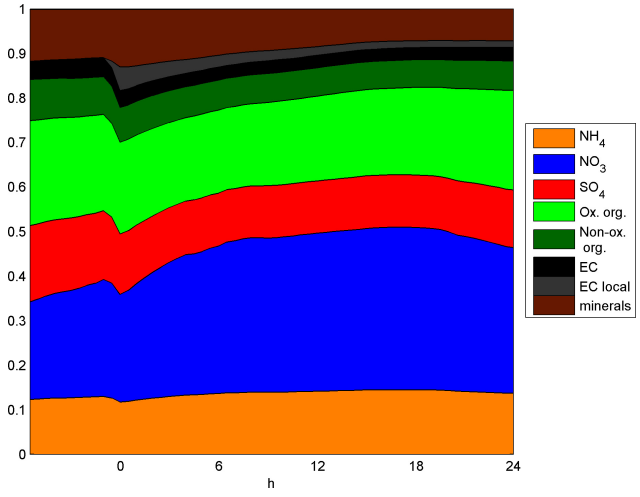

Fig. 6. Modeled average $PM_{2.5}$ mass fractions from 6 h upwind to 24 h downwind of Malmö, at the surface within the urban plume. The organic mass is divided into non-oxidized (O:C-ratio equal to zero) and oxidized material. In the model the only source for the non-oxidized organic material is low volatile POA emissions.

Figure 7 displays PM_1 mass fraction pie charts and mass size distributions of the modeled and measured chemical compounds which can be detected with ToF-AMS. Overall, the modeled PM_1 mass fractions are almost the same as the measured ones. However, the number of ammonium ions per sulfate and nitrate ion is slightly lower for the modeled values compared to the measurements, which illustrates that the AMS detected more neutralized aerosol particles than the model. The shape of the modeled mass size distributions agree with the measurements. ADCHEM is able to reproduce the larger mode diameter for the nitrate and ammonium mass size distributions compared to the organic mass size distribution. However, the measured organic mass size distribution is shifted to even smaller particles compared to the modeled total mass size distribution. Possibly, the measured organic mass size distribution is composed of a larger fraction of low volatile organic compounds than simulated in the model. This would shift the organic content to smaller particle sizes (see Fig. 8b) and discussion below). In future studies we plan to compare the AMS data inside and outside the urban plume in a similar manner to what was done with the SMPS-data.

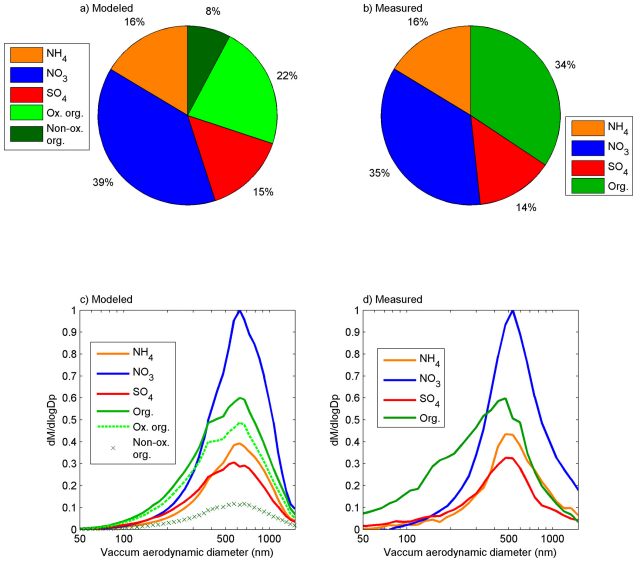

Fig. 7. Modeled (**a** and **c**) and measured (**b** and **d**) PM_1 mass fractions and mass size distributions of the compounds that can be detected with ToF-AMS. The mass size distributions were normalized with the maximum of the nitrate distributions. The chloride content was very low for the modeled and measured values and is therefore not shown. The model data is the average of the 26 model cases during 2005/2006, while the AMS data averages are from the Vavihill October and March campaigns during 2008/2009. The modeled organic mass is divided into total organics (Org.), non-oxidized (O:C-ratio equal to zero) and oxidized material. In the model the only source for the non-oxidized organic material is low volatile POA emissions.

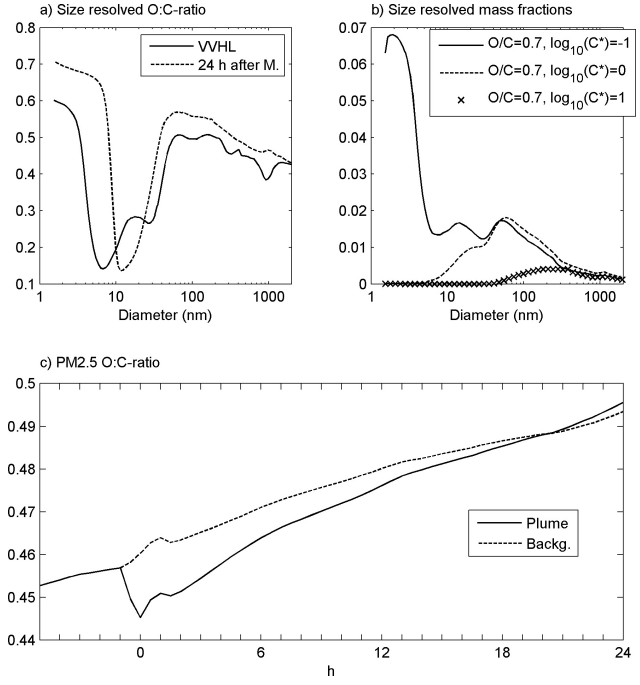

Fig. 8. Modeled organic aerosol particle properties with the 2-D-VBS model in ADCHEM. **(a)** size resolved O:C-ratio at Vavihill and 24 h downwind of Malmö, **(b)** size resolved organic aerosol mass fractions at Vavihill for three 2-D-VBS compounds with different volatility (C^*) but equal O:C-ratio and **(c)** Average $PM_{2.5}$ O:C-ratio inside and outside the urban plume downwind of Malmö.

Figure 8a shows the modeled size resolved O:C-ratio at Vavihill and 24 h downwind of Malmö. The O:C-ratios were derived with the size resolved 2-D-VBS model (see Sect. 2.2 and Roldin et al., 2011). The minimum in the O:C-ratio between 4 and 50 nm in diameter at Vavihill and 10 and 40 nm 24 h downwind of Malmö is attributed to the large influence from non-oxidized primary particle emissions within this size range. The maximum O:C-ratio is found at the smallest particle sizes where the size distribution is mainly affected by homogeneous nucleation. These particles mainly grow by condensation of low volatile organic compounds which generally have high O:C-ratios. Figure 8c gives the average $PM_{2.5}$ O:C-ratio inside and outside the urban plume downwind of Malmö. Because of the primary particle emissions in Malmö the O:C-ratio between Malmö and until 18 h downwind of the city is lower inside than outside the urban plume. Figure 8b gives an example of how condensable organic compounds with different volatility (C^*) are distributed between different particle sizes. The more volatile the compounds are the larger are the particles where these compounds are found. The reason for this is that low-volatile compounds ($C^* < 10^{-1}\,\mu g\,m^{-3}$) condense onto the Fuchs-Sutugin-corrected aerosol surface area size distribution and evaporate very slowly, while more volatile compounds ($C^* > 10^{-1}\,\mu g\,m^{-3}$) quickly condense and evaporate from the particle surfaces, until an equilibrium between the gas phase and all particle sizes is reached. Because of the Kelvin effect more volatile compounds are shifted toward larger particle sizes than less volatile compounds. This also explains why the O:C-ratio (which can be seen as a proxy for the SOA volatility) generally decreases with increasing particle size (Fig. 8a).

The secondary aerosol formation in the surface layer, formed by the anthropogenic gas phase emissions in Malmö, was estimated by taking the difference between the model results with and without anthropogenic gas phase emissions in Malmö (Fig. 9). The total $PM_{2.5}$ secondary mass contribution in the center of the model domain, downwind of Malmö, varies from -0.04 to $0.84\,\mu g\,m^{-3}$, with the maximum between 6 and 18 h downwind of Malmö. This secondary aerosol formation is dominated by condensation of nitric acid, which is neutralized by ammonium. The modeled SOA contribution due to the Malmö emissions is small compared to the ammonium nitrate formation but increases in importance with the distance from Malmö, with a maximum of $0.04\,\mu g\,m^{-3}$ at the end of the model runs 24 h downwind of Malmö. The SOA formation will likely continue to increase in importance beyond the spatial and temporal scales studied

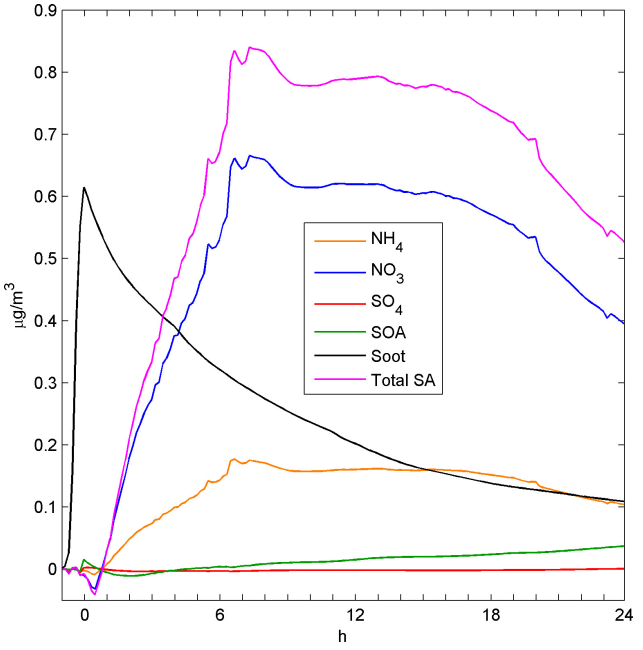

Fig. 9. Modeled average secondary aerosol (SA) formation and primary soot contribution to the $PM_{2.5}$ mass, due to gas and particle phase emissions in Malmö in the surface layer downwind of Malmö. The effective density of the soot particle emissions over Malmö was estimated to be 700 kg m^{-3}. The organic contribution only takes into account the SOA in and downwind of Malmö.

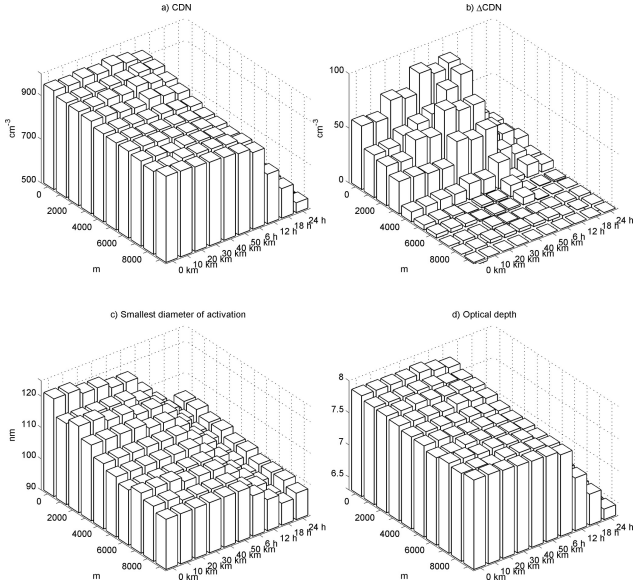

Fig. 10. Modeled cloud properties of a 100 m thick cloud, at different distances from the center of the urban plume (0–10 km) and different distances (or h) downwind of Malmö for **(a)** total Cloud Droplets Number (CDN) concentration, **(b)** number of extra cloud droplets (ΔCDN) due to the gas and particle emissions in Malmö, **(c)** the dry diameter of the smallest particles that are activated and **(d)** cloud optical depth of visible light.

in this work. The small negative secondary aerosol contribution within one hour downwind of Malmö occurs because the oxidizing capacity within the urban plume decreases (e.g. the OH and O_3 concentration decreases) and therefore BVOCs, AVOCs, SO_2 and NO_2 are oxidized more slowly within the urban plume than outside.

Figure 9 also displays the $PM_{2.5}$ soot mass contribution from the primary particle emissions in Malmö. The freshly emitted soot particles which are porous soot agglomerates were assumed to have an effective density of 700 kg m^{-3} when determining the mass emissions. This effective density agrees with measured values for diesel exhaust particles between 100 and 150 nm in diameter (Park et al., 2003). The $PM_{2.5}$ mass contribution from the soot particle emissions in Malmö decreases downwind of Malmö and more than 3 h downwind of the city the secondary aerosol mass formed from the gas phase emissions in Malmö exceeds the $PM_{2.5}$ mass contribution from soot.

3.4 Shortwave radiative forcing of the Malmö emissions

The 3-D-bar charts in Fig. 10 display modeled cloud properties for 100 m thick clouds at different distances (or h) downwind of Malmö for different distances (0–9 km) from the center of the urban plume. The cloud formation was modeled using an adiabatic cloud parcel model described in Sect. 2.9.

In Fig. 10a the total number of cloud droplets is shown, while Fig. 10b displays the number of droplets formed because of the emissions in Malmö. Initially downtown Malmö the number of cloud droplets formed from the primary particle emissions is 58 cm^{-3} (6%) higher in the center of the urban plume compared to the background, while 6 h downwind of Malmö the number of droplets reaches a maximum of 88 cm^{-3} (9%) higher at the center of the urban plume compared to the background. The increasing influence of the urban emissions on the number of cloud droplets from Malmö until 6 h downwind of Malmö are mainly due to the secondary nitrate formation. More than 6 h downwind of Malmö the modeled cloud droplet contribution due to the emissions in Malmö decreases continuously, reaching 15 cm^{-3} (3%), 24 h downwind of Malmö.

ADCHEM assumes that all particles are internally mixed, while in reality the freshly emitted soot particles in Malmö will be externally mixed in and at short distances downwind of the city. Since these externally mixed soot particles are non-water soluble they will not influence the cloud droplet number (CDN) concentration in Malmö. Therefore the modeled number of cloud droplets formed by the primary particle emissions from Malmö will most likely be overestimated in and near the city. However, more than 30 km downwind of the city the amplified CDN concentration within the urban plume is also caused by the secondary nitrate formation, and the assumption of treating the soot particles as internally mixed particles has less influence on the results.

While the number concentration of cloud droplets is higher inside than outside the urban plume, the total cloud water content is essentially the same. Hence, the geometric mean diameter (GMD) of the cloud droplets decreases with increasing number of droplets. The smallest dry particle activation diameter is also changed because of the urban emissions. In the center of the urban plume in the greater Malmö area the smallest diameter of activation is about 15 nm larger compared to the background (Fig. 10c). This is attributed to the lower water uptake of the freshly emitted primary particles in Malmö compared to the background, but also due to a lower maximum supersaturation in the more polluted clouds. Figure 10d shows the optical depth of the 100 m thick clouds downwind of Malmö. The optical depth is between 6.5 and 8 at all locations which is realistic for continental air. For these optically relatively thin clouds the cloud droplet properties have larger influence on the cloud albedo compared to thick clouds (Twomey, 1977).

The 3-D-bar charts in Fig. 11 show the calculated anthropogenic shortwave radiative forcing due to the Malmö gas and particle phase emissions at the surface without (a) and with (b) 100 m thick clouds being present at different distances (or h) downwind of Malmö and for different distances (0–9 km) from the center of the urban plume. Figure 11c and d display the radiative forcing only caused by the secondary aerosol (SA) formed from the gas phase emissions in Malmö with and without the 100 m thick clouds. Without clouds the shortwave radiative forcing in the center of the urban plume decreases with 30% from Malmö to 6 h downwind of the city (from -3.34 to $-2.31\,\mathrm{W\,m^{-2}}$), while when 100 m thick clouds are present the radiative forcing is instead increasing from $-2.4\,\mathrm{W\,m^{-2}}$ in Malmö to $-2.7\,\mathrm{W\,m^{-2}}$, 6 h downwind of the city. This can be explained by the condensation of nitric acid and ammonia (Figs. 9 and 11d), which increases the number of particles which are activated as cloud droplets (Fig. 10b). However, more than 6 h downwind of Malmö the radiative forcing decreases even when clouds are present. The reason for this is that the number of available cloud condensation nuclei (CCN) decreases due to dry and wet deposition and coagulation. Without clouds the secondary aerosol formation has insignificant influence on the radiative forcing at short distances ($\sim$ 20 km) downwind of the city. But between 6 and 24 h downwind of Malmö, when the secondary aerosol contribution from Malmö is largest (Fig. 9), the influence becomes more pronounced and explains between 10 and 20% of the total surface shortwave radiative forcing and 30 to 60% of the TOA (top of the atmosphere) shortwave radiative forcing. In contrast to the primary particle shortwave radiative forcing, which is much larger at the surface, the secondary aerosol radiative forcing is almost identical at the surface and the TOA. The reason for this is that the secondary aerosol only scatters the light while the primary particles, which mainly are composed of soot, absorb much of the solar radiation and heat the atmosphere, but still prevent the solar irradiance from reaching the surface.

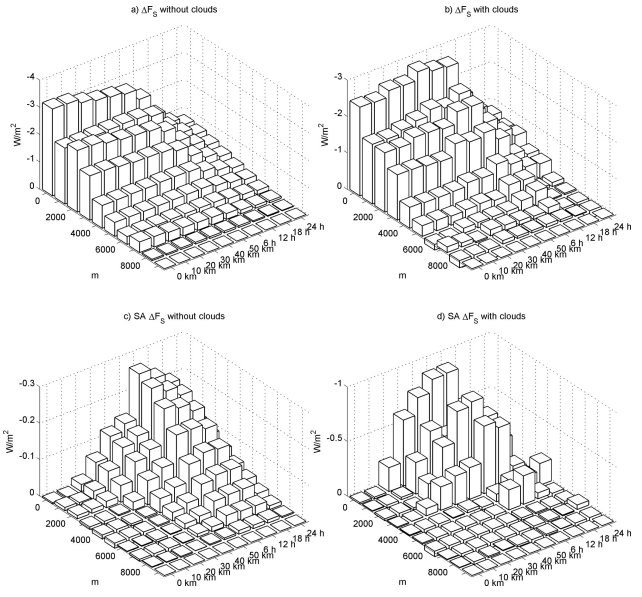

Fig. 11. Modeled anthropogenic shortwave radiative forcing at the surface due to Malmö gas and particle phase emissions at different distances (or h) downwind of Malmö and at different distances from the center of the urban plume for **(a)** conditions without clouds, **(b)** conditions with 100 m thick clouds at low altitude, **(c)** radiative forcing due to secondary aerosol (SA) formation from Malmö gas phase emissions for conditions without clouds and **(d)** same as **(c)** but with 100 m thick clouds. The secondary aerosol radiative forcing was derived by taking the difference between the modeled radiative forcing when the anthropogenic gas phase emissions from Malmö was included in the ADCHEM model and when they were not.

Table 4 displays the average radiative forcing within the 20 km wide horizontal model domain at the surface and at the TOA, at different distances (or h) downwind of Malmö with 100 m thick clouds, 500 m thick clouds or without clouds being present. At the TOA the shortwave radiative forcing is several times smaller than at the surface, especially without clouds present. If 500 m thick clouds are present instead of 100 m thick clouds the modeled shortwave radiative forcing becomes about three times smaller both at the surface and at the TOA. The reason for this is that for these much thicker clouds (optical depth between 60 and 75) the aerosol particle (cloud droplet) properties have less influence on the cloud albedo (Twomey, 1977).

It is important to remember that the average particle properties used for the radiative forcing calculations are derived from cases with southerly air masses, which generally originate from relatively polluted regions in Europe. Therefore the number of cloud droplets at the background will likely be higher compared to air masses originated over e.g. the northern part of Sweden. This condition decreases the estimated climate impact from the emissions in Malmö, especially if the emissions influence the cloud properties.

Table 4. Average radiative forcing within the 20 km wide model domain at the surface (ΔF_S) and at the TOA (ΔF_{TOA}), with or without clouds, at different distances downwind of Malmö.

Position	ΔF_S without clouds ($W\,m^{-2}$)	ΔF_S with 100 m thick clouds ($W\,m^{-2}$)	ΔF_S with 500 m thick clouds ($W\,m^{-2}$)	ΔF_{TOA} without cloud ($W\,m^{-2}$)	ΔF_{TOA} with 100 m thick clouds ($W\,m^{-2}$)	ΔF_{TOA} with 500 m thick clouds ($W\,m^{-2}$)
Malmö	−1.147	−0.762	−0.221	−0.262	−0.289	−0.107
10 km dw. M	−1.113	−0.743	−0.215	−0.237	−0.271	−0.101
20 km dw. M	−1.08	−0.784	−0.245	−0.219	−0.322	−0.129
30 km dw. M	−1.053	−0.851	−0.271	−0.207	−0.397	−0.153
40 km dw. M	−1.047	−0.922	−0.300	−0.204	−0.471	−0.179
50 km dw. M	−1.026	−0.908	−0.297	−0.200	−0.465	−0.178
6 h dw. M.	−0.931	−0.999	−0.337	−0.185	−0.600	−0.222
12 h dw. M.	−0.652	−0.747	−0.314	−0.169	−0.479	−0.225
18 h dw. M.	−0.467	−0.413	−0.159	−0.139	−0.227	−0.105
24 h dw. M.	−0.346	−0.295	−0.102	−0.101	−0.153	−0.062

3.5 Health effects of the ageing urban aerosol

It could be noted that in addition to the effects on the radiation balance, the alteration in chemical and physical properties of the aerosol during its ageing has an impact on human health. For instance there may be a difference in toxicity between the fresh and the aged aerosol because of variations in concentration and ability of the particles to deposit in the human lungs. The fresh aerosol contains a larger proportion of ultrafine particles with a high probability to deposit in the lungs and by number the amount of deposited particles will thus be high compared to that for the aged aerosol. On the other hand the increase in mass and the shift in hygroscopicity of the aged aerosol results in a higher particle deposition in the lungs by mass. This kind of lung deposition estimates can be derived using the results from the ADCHEM model.

4 Summary and conclusions

In this work a coupled aerosol dynamics, gas phase chemistry and radiative transfer model (ADCHEM) has been used first, to test if it can correctly model an ageing urban plume, in this case generated by Malmö, a city with 280 000 inhabitants in Southern Sweden. However, the main objective has been to use ADCHEM to estimate the climate impacts of the ageing plume.

ADCHEM was able to accurately model the ageing of the particle number size distribution for 26 different case studies between an urban background site in Malmö and the rural site Vavihill, 50 km downwind of Malmö. At Vavihill, the model results were validated with particle number size distribution measurements. The differences between average modeled and measured concentrations of O_3, NO, NO_2 and SO_2 in Malmö were smaller than 25%. Hence, the model is able to capture the main features of the gas phase chemistry in the Malmö plume, which is required to be able to accurately predict the secondary aerosol formation.

The modeled inorganic and organic particle composition is comparable with ToF-AMS measurements at Vavihill. This illustrates that ADCHEM can be used to model realistic size-resolved particle chemical composition in urban plumes, and that the model results can further be used to calculate the optical and hygroscopic properties relevant for climate and health effects.

Malmö contributes with about 1200 particles cm^{-3} at Vavihill, where the number concentration is dominated by primary emissions in the nucleation and Aitken mode. While the primary particle number contribution continuously decreases downwind of the emission sources, the contribution to the aerosol particle mass from secondary aerosol formation continues to increase up to several hundred kilometers ($\sim$ 12 h) downwind of Malmö. The secondary aerosol formation is dominated by condensation of nitric acid, formed from the NO_x emissions in Malmö. The maximum secondary aerosol contribution from the gas phase emissions in Malmö of between 0.7 and 0.8 $\mu g\,m^{-3}$ in the urban plume is reached between 6 and 18 h downwind of Malmö.

The secondary aerosol formation downwind of Malmö leads to growth of the freshly emitted primary particles, which results in a more hygroscopic aerosol. This increases its impact on the cloud properties within the urban plume. Hence, the cloud radiative forcing due to the emissions in Malmö is largest about 40–200 km ($\sim$ 2–12 h) downwind of Malmö and not within or very near the city.

Because 60% of the world population lives in cities with less than 1 million people, i.e. of the same size as Malmö, the climate and health impact of these cities need to be addressed. The urban emission contribution downwind of the city center estimated from this study can be used for up-scaling of urban sub-grid emissions to regional scales treated by global and regional chemistry transport models

and climate models. The results can further be used to estimate how the particle emissions influence adjacent grid cells of these models. However, since the meteorological conditions, emission sources, and geographical and population extension vary between different cities, more detailed studies of different urban regions around the world are needed to better account for their influence on climate and population health on regional and global scales.

Nevertheless, this study has shown that it is not sufficient to account only for aerosol dynamic processes during the transformation of local scale anthropogenic emissions to larger scales of regional and global models. Gas-phase chemistry and secondary aerosol formation are necessary entities to account for during the prediction of climate and health effects of particles in the ageing urban plumes.

Supplementary material related to this article is available online at: http://www.atmos-chem-phys.net/11/5897/2011/acp-11-5897-2011-supplement.pdf.

Acknowledgements. This work has been supported by the European Commission 6th Framework program projects: EUCAARI, contract no 036833-2 (EUCAARI) and EUSAAR, contract no 026140 (EUSAAR). We also gratefully acknowledge the support by the Swedish Research Council through project no 2007-4619, the Swedish strategic research area ModElling the Regional and Global Earth system, MERGE and the Lund University center for studies of Carbon cycle and Climate Interactions, LUCCI. The Swedish Research Council also funded the purchase of the HR-ToF-AMS instrument through Research Equipment Grant no 2006-5940. The DMPS measurements at Vavihill were supported by the Swedish Environmental Protection Agency within the Swedish Environmental Monitoring Program. The support by the Swedish Research Council for Environment, Agricultural Sciences and Spatial Planning (Formas) through project no 2009-615 and 2008-1467 is also gratefully acknowledged.

The authors would also like to thank Almut Arneth and Guy Schurgers at Department of Earth and Ecosystem Sciences, Lund University, for providing BVOC emissions over Europe, Harri Kokkola, Joni-Pekka Pietikäinen and Jussi Malila at Kuopio University, for valuable help during the development of the adiabatic cloud parcel model, Henrik Nilsson at Environmental Dept., City of Malmö for the gas and wind direction measurements in Malmö, Tareq Hussein from Helsinki University for help with the lognormal-fitting of the measured and modeled particle number size distributions, Matthias Ketzel and Fenjuan Wang from Danish National Environmental Research Institute for help with the implementation of the Danish anthropogenic gas and particle phase emissions and David Simpson at the Global Environmental Measurement and Modelling Group, Department of Radio and Space Science, Chalmers, Gothenburg for help with the SOA partitioning theory.

Edited by: A. Wiedensohler

References

Arneth, A., Niinemets, Ü, Pressley, S., Bäck, J., Hari, P., Karl, T., Noe, S., Prentice, I. C., Serça, D., Hickler, T., Wolf, A., and Smith, B.: Process-based estimates of terrestrial ecosystem isoprene emissions: incorporating the effects of a direct CO_2-isoprene interaction, Atmos. Chem. Phys., 7, 31–53, doi:10.5194/acp-7-31-2007, 2007.

Chaix, B., Gustafsson, S., Jerrett, M., Kristersson, H., Lithman, T., Boalt, Å., and Merlo, J.: Children's exposure to nitrogen dioxide in Sweden: investigating environmental injustice in an egalitarian country, J. Epidemiol. Comm. H., 60, 234–241, 2006.

Doran, J. C., Barnard, J. C., Arnott, W. P., Cary, R., Coulter, R., Fast, J. D., Kassianov, E. I., Kleinman, L., Laulainen, N. S., Martin, T., Paredes-Miranda, G., Pekour, M. S., Shaw, W. J., Smith, D. F., Springston, S. R., and Yu, X.-Y.: The T1-T2 study: evolution of aerosol properties downwind of Mexico City, Atmos. Chem. Phys., 7, 1585–1598, doi:10.5194/acp-7-1585-2007, 2007.

Draxler, R. R. and Rolph, G. D.: HYSPLIT (Hybrid Single-Particle Lagrangian Integrated Trajectory) Model, available at: http://ready.arl.noaa.gov/HYSPLIT.php, NOAA Air Resources Laboratory, Silver Spring, MD, (last access: 01 March 2011) 2011.

Eriksson, A.: Calibration and First Field Deployment of an Aerosol Mass Spectrometer, M. Sc dissertation at Department of Physics and Department of Design Sciences, Lund University, 2009.

Gaydos, T. M., Pinder, R., Koo, B., Fahey, K. M., Yarwood, G., and Pandis, S. N.: Development and application of a three-dimensional aerosol chemical transport model, PMCAMx, Atmos. Environ., 41, 2594–2611, 2007.

Gustafsson, S.: Uppbyggnad och validering av emissionsdatabas avseende luftföroreningar för Skåne med basår, Licentiat Dissertation at National Environmental Research Institute, Lund University, 9, 2001.

Henze, D. K., Seinfeld, J. H., Ng, N. L., Kroll, J. H., Fu, T.-M., Jacob, D. J., and Heald, C. L.: Global modeling of secondary organic aerosol formation from aromatic hydrocarbons: high-vs. low-yield pathways, Atmos. Chem. Phys., 8, 2405–2420, doi:10.5194/acp-8-2405-2008, 2008.

Hodzic, A., Vautard, R., Chazette, P., Menut, L., and Bessagnet, B.: Aerosol chemical and optical properties over the Paris area within ESQUIF project, Atmos. Chem. Phys., 6, 3257–3280, doi:10.5194/acp-6-3257-2006, 2006.

Hodzic, A., Jimenez, J. L., Madronich, S., Aiken, A. C., Bessagnet, B., Curci, G., Fast, J., Lamarque, J.-F., Onasch, T. B., Roux, G., Schauer, J. J., Stone, E. A., and Ulbrich, I. M.: Modeling organic aerosols during MILAGRO: importance of biogenic secondary organic aerosols, Atmos. Chem. Phys., 9, 6949–6981, doi:10.5194/acp-9-6949-2009, 2009.

Horvath, H.: Influence of atmospheric aerosols upon the global radiation balance, in: Atmospheric Particles IUPAC Series on Analytical and Physical Chemistry of Environmental Systems, edited by: Harrison, R. M. and Van Greiken, R., Wiley, New York, 5, 1998.

Hussein, T., Dal Maso, M., Petaja, T., Koponen, I. K., Paatero, P., Aalto, P. P., Hämeri, K., and Kulmala, M.: Evaluation of an automatic algorith for fitting the particle number size distributions, Boreal Environ. Res., 10, 337–355, 2005.

Jacobson, M. Z.: A Solution to the Problem of Nonequilibrium

Acid/Base Gas-Particle Transfer at Long Time Step, Aerosol Sci. Tech., 39, 92–103, 2005a.

Jacobson, M. Z.: Fundamentals of Atmospheric Modelling, 2nd Edn., Cambridge University Press, Cambridge, United Kingdom and New York, NY, USA, 2005b.

Jimenez, J. L., Canagaratna, M. R., Donahue, N. M., Prevot, A. S. H., Zhang, Q., Kroll, J. H., DeCarlo, P. F., Allan, J. D., Coe, H., Ng, N. L., Aiken, A. C., Docherty, K. S., Ulbrich, I. M., Grieshop, A. P., Robinson, A. L., Duplissy, J., Smith, J. D., Wilson, K. R., Lanz, V. A., Hueglin, C., Sun, Y. L., Tian, J., Laaksonen, A., Raatikainen, T., Rautiainen, J., Vaattovaara, P., Ehn, M., Kulmala, M., Tomlinson, J. M., Collins, D. R., Cubison, M. J., Dunlea, E. J., Huffman, J. A., Onasch, T. B., Alfarra, M. R., Williams, P. I., Bower, K., Kondo, Y., Schneider, J., Drewnick, F., Borrmann, S., Weimer, S., Demerjian, K., Salcedo, D., Cottrell, L., Griffin, R., Takami, A., Miyoshi, T., Hatakeyama, S., Shimono, A., Sun, J. Y, Zhang, Y. M., Dzepina, K., Kimmel, J. R., Sueper, D., Jayne, J. T., Herndon, S. C., Trimborn, A. M., Williams, L. R., Wood, E. C., Middlebrook, A. M., Kolb, C. E., Baltensperger, U., and Worsnop, D. R.: Evolution of Organic Aerosols in the Atmosphere, Science, 326, 1525–1529, 2009.

Kristensson, A., Dal Maso, M., Swietlicki, E., Hussein, T., Zhou, J., Kerminen, V.-M., and Kulmala, M.: Characterization of new particle formation events at a background site in Southern Sweden: relation to air mass history, Tellus, 60B, 330–344, 2008.

Ng, N. L., Kroll, J. H., Chan, A. W. H., Chhabra, P. S., Flagan, R. C., and Seinfeld, J. H.: Secondary organic aerosol formation from *m*-xylene, toluene, and benzene, Atmos. Chem. Phys., 7, 3909–3922, doi:10.5194/acp-7-3909-2007, 2007.

Nolte, C. G., Bhave, P. V., Arnold, J. R., Dennis, R. L., Zhang, K. M., and Wexler, A. S.: Modeling urban and regional aerosols-Application of the CMAQ-UCD Aerosol Model to Tampa, a coastal urban site, Atmos. Environ., 42, 3179–3191, 2008.

Odum, J. R., Hoffmann, T., Bowman, F., Collins, D., Flagan, R. C., and Seinfeld, J. H.: Gas/Particle Partitioning and Secondary Organic Aerosol Yields, Environ. Sci. Technol., 30, 2580–2585, 1996.

Park, K., Cao, F., Kittelson, D. B., and McMurry, P. H.: Relationship between Particle Mass and Mobility for Diesel Exhaust Particles, Environ. Sci. Technol., 37, 577–583, 2003.

Patashnick, H. and Rupprecht, E. G.: Continuous PM_10 measurements using the tapered element oscillating microbalance, J. Air Waste Manage. Ass., 41, 1079–1083, 1991.

Pierce, J. R., Theodoritsi, G., Adams, P. J., and Pandis, S. N.: Parameterization of the effect of sub-grid scale aerosol dynamics on aerosol number emission rates, Aerosol Sci., 40, 385–393, 2009.

Pirjola, L. and Kulmala, M.: Modelling the formation of H_2SO_4-H_2O particles in rural, urban and marine conditions, Atmos. Res., 46, 321–347, 1998.

Population Division of the Department of Economic and Social Affairs of the United Nations Secretariat, World Population Prospects: The 2006 Revision and World Urbanization Prospects: The 2007 Revision, available at: http://esa.un.org/unup (last acess: 01 March 2011), 2007.

Ramankutty, N., Evan, A. T., Monfreda, C., and Foley, J. A.: Farming the planet: 1. Geographic distribution of global agricultural lands in the year 2000, Global Biogeochem. Cy., 22, GB1003, doi:10.1029/2007GB002952, 2008.

Robinson, A. L., Donahue, N. M., Shrivastava, M. K., Weitkamp, E. A., Sage, A. M., Grieshop, A. P., Lane, T. E., Pierce, J. R., and Pandis, S. N.: Rethinking organic aerosols: Semivolatile emissions and photochemical aging, Science, 315, 1259–1262, 2007.

Rogers, R. R. and Yau, M. K.: A Short Course in Cloud Physics, 3rd Edn., Pergamon Press, Oxford, Great Britain, 1989.

Rolph, G. D.: Real-time Environmental Applications and Display sYstem (READY), NOAA Air Resources Laboratory, Silver Spring, MD, available at: http://ready.arl.noaa.gov/, 2011.

Roldin, P., Swietlicki, E., Schurgers, G., Arneth, A., Lehtinen, K. E. J., Boy, M., and Kulmala, M.: Development and evaluation of the aerosol dynamics and gas phase chemistry model ADCHEM, Atmos. Chem. Phys., 11, doi:10.5194/acp-11-5867-2011, 5867–5896, 2011.

Seinfeld, J. H., Carmichael, G. R., Arimoto, R., Conant, W. C., Brechtel, F. J., Bates, T. S., Cahill, T. A., Clarke, A. D., Doherty, S. J., Flatau, P. J., Huebert, B. J., Kim, J., Markowicz, K. M., Quinn, P. K., Russell, L. M., Russell, P. B., Shimizu, A., Shinozuka, Y., Song, C. H., Tang, Y., Uno, I., Vogelmann, A. M., Weber, R. J., Woo, J.-H., and Zhang, X. Y.: ACE-ASIA – Regional Climatic and Atmospheric Chemical Effects of Asian Dust and Pollution, Bull. Am. Meteorol. Soc, 85, 367–380, 2004.

Schmid, O., Chand, D., Karg, E., Guyon, P., Frank, G. P., Swietlicki, E., and Andreae, M. O.: Derivation of the Density and Refractive Index of Organic Matter and Elemental Carbon from Closure between Physical and Chemical Aerosol Properties, Environ. Sci. Technol., 43, 1166–1172, 2009.

Schurgers, G., Arneth, A., Holzinger, R., and Goldstein, A. H.: Process-based modelling of biogenic monoterpene emissions combining production and release from storage, Atmos. Chem. Phys., 9, 3409–3423, doi:10.5194/acp-9-3409-2009, 2009.

Shrivastava, M. K., Lane, T. E., Donahue, N. M., Pandis, S. N., and Robinson, A. L.: Effects of gas particle partitioning and aging of primary emissions on urban and regional organic aerosol concentrations, J. Geophys. Res., 113, D18301, doi:10.1029/2007JD009735, 2008.

Simpson, D., Winiwarter, W., Börjesson, G., Cinderby, S., Ferreiro, A., Guenther, A., Hewitt, N., Janson, R., Khalil, M. A. K., Owen, S., Pierce, T. E., Puxbaum, H., Shearer, M., Skiba, U., Steinbrecher, R., Tarrasón, L., and Öquist, M. G.: Inventorying emissions from nature in Europe, J. Geophys. Res., 104, 8113–8152, 1999.

Sitch, S., Smith, B., Prentice, I., Arneth, A., Bondeau, A., Cramer, W., Kaplan, J., Levis, S., Lucht, W., Sykes, M., Thonicke, K., and Venevsky, S.: Evaluation of ecosystem dynamics, plant geography and terrestrial carbon cycling in the LPJ Dynamic Global Vegetation Model, Glob. Change Biol., 9, 161–185, 2003.

Smith, B., Prentice, I. C., and Sykes, M. T.: Representation of vegetation dynamics in the modeling of terrestrial ecosystems: comparing two contrasting approaches within European climate space, Glob. Ecol. Biogeogr., 10, 621–637, 2001.

Sokolik, I. N. and Toon, O. B.: Incorporation of mineralogical composition into models of radiative properties of mineral aerosol from UV to IR wavelength, J. Geophys. Res., 104, 9423–9444, 1999.

Stroh, E., Harrie, L., and Gustafsson, S.: A study of spatial resolution in pollution exposure modeling, Int. J. Health Geogr., 6(1), 19–19, doi:10.1186/1476-072X-6-19, 2007.

Tie, X., Madronich, S., Li, G., Ying, Z., Weinheimer, A., Apel, E., and Campos, T.: Simulation of Mexico City plumes during the

MIRAGE-Mex field campaign using the WRF-Chem model, Atmos. Chem. Phys., 9, 4621–4638, doi:10.5194/acp-9-4621-2009, 2009.

Toon, O. B., McKay, C. P., Ackerman, T. P., and Santhanam, K.: Rapid Calculation of Radiative Heating Rates and Photodissociation Rates in Inhomogeneous Multiple Scattering Atmospheres, J. Geophys. Res., 94, 16287–16301, 1989.

Tsimpidi, A. P., Karydis, V. A., Zavala, M., Lei, W., Molina, L., Ulbrich, I. M., Jimenez, J. L., and Pandis, S. N.: Evaluation of the volatility basis-set approach for the simulation of organic aerosol formation in the Mexico City metropolitan area, Atmos. Chem. Phys., 10, 525–546, doi:10.5194/acp-10-525-2010, 2010.

Twomey, S.: The Influence of Pollution on the Shortwave Albedo of Clouds, J. Atmos. Sci., 34, 1149–1152, 1977.

Vestreng, V., Rigler, E., Adams, M., Kindbom, K., Pacyna, J. M., van der Gon, D., Reis, H. S., and Traynikov, O.: Inventory review 2006, Emission data reported to LRTAP and NEC Directive, Stage 1, 2 and 3 review and Evaluation of Inventories of HM and POPs, EMEP/MSC-W Technical Report 1/2006, 1504–6179, available at: http://www.emep.int/, 2006.

Wang, F., Roldin, P., Massling, A., Kristensson, A., Swietlicki, E., Fang, D., and Ketzel, M.: Aerosol dynamics in the Copenhagen urban plume during regional transport, Atmos. Chem. Phys. Discuss., 10, 8553–8594, doi:10.5194/acpd-10-8553-2010, 2010.

Wiedensohler, A., Birmili, W., Nowak, A., Sonntag, A., Weinhold, K., Merkel, M., Wehner, B., Tuch, T., Pfeifer, S., Fiebig, M., Fjäraa, A. M., Asmi, E., Sellegri, K., Depuy, R., Venzac, H., Villani, P., Laj, P., Aalto, P., Ogren, J. A., Swietlicki, E., Roldin, P., Williams, P., Quincey, P., Hüglin, C., Fierz-Schmidhauser, R., Gysel, M., Weingartner, E., Riccobono, F., Santos, S., Grüning, C., Faloon, K., Beddows, D., Harrison, R. M., Monahan, C., Jennings, S. G., O'Dowd, C. D., Marinoni, A., Horn, H.-G., Keck, L., Jiang, J., Scheckman, J., McMurry, P. H., Deng, Z., Zhao, C. S., Moerman, M., Henzing, B., and de Leeuw, G.: Particle mobility size spectrometers: harmonization of technical standards and data structure to facilitate high quality long-term observations of atmospheric particle number size distributions, Atmos. Meas. Tech. Discuss., 3, 5521–5587, doi:10.5194/amtd-3-5521-2010, 2010.

Winklmayr, W., Reischl, G. P., Lindner, A. O., and Berner, A.: A new electromobility spectrometer for the measurement of aerosol size distributions in the size range from 1 to 1000 nm, J. Aerosol Sci., 22, 289–296, 1991.

Zaveri, R. A., Easter, R. C., Fast, J. D., and Peters, L. K.: Model for Simulating Aerosol Interactions and Chemistry (MOSAIC), J. Geophys. Res., 113, D13204, doi:10.1029/2007JD008782, 2008.

Zhang, K. M. and Wexler, A. S.: Modeling urban and regional aerosols-Development of the UCD Aerosol Module and implementation in CMAQ model, Atmos. Environ., 42, 3166–3178, 2008.